Maastricht University

Local bone metabolism during the consolidation process of spinal interbody fusion

Citation for published version (APA):

Loenen, A. C. Y., Peters, M. J. M., Wierts, R., Bevers, R. T. J., van Rhijn, L. W., Arts, J. J., & Willems, P. C. (2022). Local bone metabolism during the consolidation process of spinal interbody fusion. *Journal of Bone and Mineral Metabolism*, *40*(2), 220-228. https://doi.org/10.1007/s00774-021-01281-8

Document status and date:
Published: 01/03/2022

DOI:
10.1007/s00774-021-01281-8

Document Version:
Publisher's PDF, also known as Version of record

Document license:
Taverne

Please check the document version of this publication:

• A submitted manuscript is the version of the article upon submission and before peer-review. There can be important differences between the submitted version and the official published version of record. People interested in the research are advised to contact the author for the final version of the publication, or visit the DOI to the publisher's website.
• The final author version and the galley proof are versions of the publication after peer review.
• The final published version features the final layout of the paper including the volume, issue and page numbers.

Link to publication

General rights
Copyright and moral rights for the publications made accessible in the public portal are retained by the authors and/or other copyright owners and it is a condition of accessing publications that users recognise and abide by the legal requirements associated with these rights.

• Users may download and print one copy of any publication from the public portal for the purpose of private study or research.
• You may not further distribute the material or use it for any profit-making activity or commercial gain
• You may freely distribute the URL identifying the publication in the public portal.

If the publication is distributed under the terms of Article 25fa of the Dutch Copyright Act, indicated by the “Taverne” license above, please follow below link for the End User Agreement:

www.umlib.nl/taverne-license

Take down policy
If you believe that this document breaches copyright please contact us at:

repository@maastrichtuniversity.nl

providing details and we will investigate your claim.

Download date: 06 Nov. 2022

Journal of Bone and Mineral Metabolism
https://doi.org/10.1007/s00774-021-01281-8

ORIGINAL ARTICLE

Local bone metabolism during the consolidation process of spinal interbody fusion

Arjan C. Y. Loenen[1,2] · Marloes J. M. Peters[1] · Roel Wierts[3] · Raymond T. J. Bevers[1] · Lodewijk W. van Rhijn[1] · Jacobus J. Arts[1,2] · Paul C. Willems[1]

Received: 26 July 2021 / Accepted: 14 October 2021
© The Japanese Society Bone and Mineral Research 2021

Abstract

Introduction Although computed tomography (CT) can identify the presence of eventual bony bridges following lumbar interbody fusion (LIF) surgery, it does not provide information on the ongoing formation process of new bony structures. ^{18}F sodium fluoride (^{18}F-NaF) positron emission tomography (PET) could be used as complementary modality to add information on the bone metabolism at the fusion site. However, it remains unknown how bone metabolism in the operated segment changes early after surgery in uncompromised situations. This study aimed to quantify the changes in local bone metabolism during consolidation of LIF.

Materials and methods Six skeletally mature sheep underwent LIF surgery. ^{18}F-NaF PET/CT scanning was performed 6 and 12 weeks postoperatively to quantify the bone volume and metabolism in the operated segment. Bone metabolism was expressed as a function of bone volume.

Results Early in the fusion process, bone metabolism was increased at the endplates of the operated vertebrae. In a next phase, bone metabolism increased in the center of the interbody region, peaked, and declined to an equilibrium state. During the entire postoperative time period of 12 weeks, bone metabolism in the interbody region was higher than that of a reference site in the spinal column.

Conclusion Following LIF surgery, there is a rapid increase in bone metabolism at the vertebral endplates that develops towards the center of the interbody region. Knowing the local bone metabolism during uncompromised consolidation of spinal interbody fusion might enable identification of impaired bone formation early after LIF surgery using ^{18}F-NaF PET/CT scanning.

Keywords Lumbar interbody fusion · Ovine · ^{18}F sodium fluoride positron emission tomography · Computed tomography · Bone metabolism

Introduction

Lumbar interbody fusion (LIF) can be used as operative treatment for a wide range of spinal disorders if conservative treatment has failed [1]. LIF aims to stabilize a painful intervertebral segment by stimulating a bony bridge between the two adjacent vertebral bodies. Following resection of the intervertebral disc and preparation of the endplates, an interbody cage filled with bone graft or bone graft substitute is inserted [2, 3]. The treatment relies on bony union of the two adjacent vertebrae through the cage for long-term success [4, 5].

Meng et al. reported that up to 20% of LIFs do not result in bony union between the vertebrae of the operated segment [3]. Non-unions are not symptomatic by definition, but

✉ Paul C. Willems
p.willems@mumc.nl

1 Laboratory for Experimental Orthopaedics, Department of Orthopaedic Surgery, CAPHRI, Maastricht University Medical Center, Maastricht, The Netherlands

2 Orthopaedic Biomechanics, Department of Biomedical Engineering, Eindhoven University of Technology, Eindhoven, The Netherlands

3 Department of Radiology and Nuclear Medicine, Maastricht University Medical Center, Maastricht, The Netherlands

Published online: 10 November 2021

are generally correlated with inferior clinical outcome [4, 6]. The symptoms secondary to a non-union mainly emerge on mid- and long-term follow-up and may require revision surgery up to 10 years after the initial treatment [7]. It is, therefore, important to predict symptomatic non-unions as soon as possible. Surgical exploration is considered the gold standard to evaluate bony union, whereas computed tomography (CT) is considered as the most reliable non-invasive modality [8]. CT is typically used to classify the fusion success based on the presence of mineralized bony bridges between vertebrae throughout the disc space [9]. Although CT provides excellent details on the current presence of osseous structures at the fusion site (diagnostic information), it does not provide information on local bone remodeling activity and whether uncompromised progression of fusion is to be expected (prognostic information).

Positron emission tomography (PET) with the bone seeking tracer ^{18}F sodium fluoride (^{18}F-NaF) has been previously proposed as a complementary modality to provide quantitative information on local bone metabolism in the operated spine [10–12]. ^{18}F-NaF tracer uptake is known to increase within skeletal tissue with increasing perfusion, vascular permeability, bone turnover, and amount of exposed mineral surface [13, 14]. Therefore, increased tracer uptake corresponds with increased bone metabolism. Persistently increased bone metabolism more than 1 year after LIF has been reported to originate from micro-instability and increased tissue stresses at the interface of the cage and has previously been identified as indicator for impaired bone graft healing and painful non-union [11, 15].

In operated segments in which a bony fusion is successfully consolidating, interbody bone metabolism is expected to strongly increase early after surgery because of active new bone formation in the interbody region [16]. On the longer term (years), however, interbody bone metabolism is expected to approach the bone metabolism of mature bone i.e. a bone metabolism corresponding with maintenance of bone homeostasis without any signs of under- or overloading of the bone. However, it remains elusive how the interbody bone metabolism transitions from low intensity (there is no bone metabolism in the intervertebral disc space before surgery), towards strongly increased intensity (early after surgery), towards a homeostatic intensity (long after surgery), and how these changes in metabolism relate to the status and quality of fusion of the operated segment.

To properly interpret PET signals and assess their relevance in clinical research, it is important to understand the changes in local bone metabolism following LIF and how this relates to the status of fusion. Therefore, the objective of this study was to quantify the changes in local bone metabolism during the consolidation process of interbody fusion. A preclinical ovine cohort that was subjected to LIF surgery was longitudinally monitored by ^{18}F-NaF PET/CT scanning. The status of interbody fusion in the cages was quantified per scan in a standardized way using CT data, whereas local bone metabolism was quantified in the interbody and endplate regions based on normalized ^{18}F-NaF uptake values. Normalized ^{18}F-NaF uptake values were generated per scan by dividing the activity value of every voxel by the mean activity of an internal reference site in the spinal column. To evaluate the changes in local bone metabolism during the consolidation process of fusion, normalized tracer uptake was expressed as a function of fusion status.

Materials and methods

Animal model and study design

Six skeletally mature Zwartbles ewes (age 2–4 years, weight 76–112 kg) were included from an existing ovine cohort on LIF surgery with a scheduled postoperative time period of 13 weeks [17]. Sheep underwent LIF by insertion of a polyether ether ketone (PEEK) cage filled with autologous iliac crest bone graft (ICBG) at either level L2–L3 or L4–L5. The PEEK cages were custom designed and manufactured (Instrument Development, Engineering and Evaluation, Maastricht University, Maastricht, the Netherlands) to fit the vertebrae of the sheep. Cages were $22 \times 9 \times 6$ mm^3 in size, contained titanium markers, and had a central graft window of approximately 0.5 mL. All animal protocols were conducted in accordance with the European directive 2010/63/EU and were approved by local animal welfare committees at the involved institutions in Belgium (Medanex Clinic, Diest; EC MxCl 2018–110) and the Netherlands (Maastricht University, Maastricht; AVD1070020185685).

Surgical technique and postoperative course

Surgery on the sheep was performed by an experienced spine surgeon (PW) at the Medanex Clinic (Diest, Belgium) under general anesthesia with endotracheal intubation with the animal in the right lateral decubitus position. Following a retroperitoneal approach of the designated intervertebral disc space and fluoroscopic confirmation, discectomy and endplate rasping was performed. Customized rasp tools that gradually increased in height up to 5 mm enabled revascularization of the endplates and preparation of the intervertebral space for cage impaction. At the caudal side of the incision, the cortical shell of the iliac crest was exposed and opened to harvest ICBG. The cage graft window was filled with the autologous ICBG before impaction. Additional instrumentation could be omitted because the 6 mm high cages were tightly compressed by the two adjacent vertebrae. The wound was closed layer-by-layer using appropriate sutures.

After complete recovery from surgery, the sheep were transported from the Medanex Clinic (Diest, Belgium) to the animal facility of Maastricht University (Maastricht, the Netherlands) for PET/CT scanning at six and 12 weeks after surgery. The sheep were group housed, were free to move throughout the follow-up period, and had ad libitum access to hay and water. After 13 weeks, the sheep were euthanized and the operated intervertebral segments were isolated for histology.

PET/CT acquisition

The sheep were scanned under general anesthesia in a Discovery MI 5 ring PET/CT system (GE Healthcare, Milwaukee, WI, USA). Thirty minutes after intravenous injection of 1.2–2.4 MBq ^{18}F-NaF tracer per kilogram body weight, a low-dose CT (120 kV, 20 mAs, slice thickness 2.5 mm) was acquired, which was used for attenuation correction upon reconstruction of the positron emission signals. PET acquisition of the complete lumbar spine was performed using a single bed position with an acquisition time of 10 min. Directly after PET acquisition, a diagnostic CT (140 kV, 300 mAs, slice thickness 1.25 mm with increment of 0.625 mm) of the lumbar spine was made. Standard filtered back projection was performed to reconstruct CT images as 512 × 512 matrices. Attenuation-corrected PET images were reconstructed as 256 × 256 matrices with a block sequential regularized expectation maximization algorithm including time-of-flight and point spread functions (commercial name Q.Clear, GE Healthcare, Milwaukee, WI, USA) [18]. The penalization factor of this iterative reconstruction algorithm (termed beta) was set to 700.

Quantification of fusion based on diagnostic CT data

The diagnostic CT images were used to quantify the status of interbody fusion of the PEEK segments for each sheep at both 6 and 12 weeks after surgery. Images were analyzed using medical image processing software (Mimics version 22.0, Materialise, Leuven, Belgium). For visualization purposes, the brightness and contrast settings of the grayscale were standardized across all images using the Hounsfield units (HUs). For every scan, the titanium markers of the customized PEEK cage were segmented by thresholding (HU > 1000). Then, the computer aided design file describing the PEEK cage including titanium markers and central graft window was imported into the software. To position the design file correctly within each CT scan, the cage was automatically repositioned by aligning the titanium markers of the design file with the segmented titanium markers from the scan (Fig. 1). To yield a percentage of bone volume for every scan in a standardized manner, the bone was quantified (HU > 500) within and normalized to the central graft window of the cage.

Quantification of ^{18}F-NaF uptake

The CT and corresponding attenuation-corrected PET images were imported into dedicated research software (PMOD version 4.1, PMOD Technologies, Zürich, Switzerland) to quantify ^{18}F-NaF uptake. A volume of interest (VOI) with an axial height of 30 mm, surrounding the vertebral bodies of L5 and L6, was centered on intervertebral disc L5–L6, and was thresholded for bone (HU > 250). This resulted in a reference VOI (VOI_{REF}) per scan (Fig. 2, upper row) of 15–20 mL in volume. For each scan, the mean ^{18}F-NaF uptake in the VOI_{REF} was derived in kBq/mL from corresponding attenuation-corrected PET images. This value was subsequently used to normalize the PET images with an internal reference value, i.e. each voxel ^{18}F-NaF uptake value (in kBq/mL) was divided by the mean ^{18}F-NaF uptake value of the VOI_{REF} (in kBq/mL) of the scan.

On the axial slices of each CT, VOIs were manually drawn in the center of the operated interbody segment (VOI_{IB}) and at the endplates above and below (VOI_{EP}). These VOIs were all 3.75 mm in axial height and surrounded the original contours of vertebral bodies in the axial plane. VOI_{IB} and VOI_{EP} were 2.0–2.7 and 1.7–2.6 mL in volume,

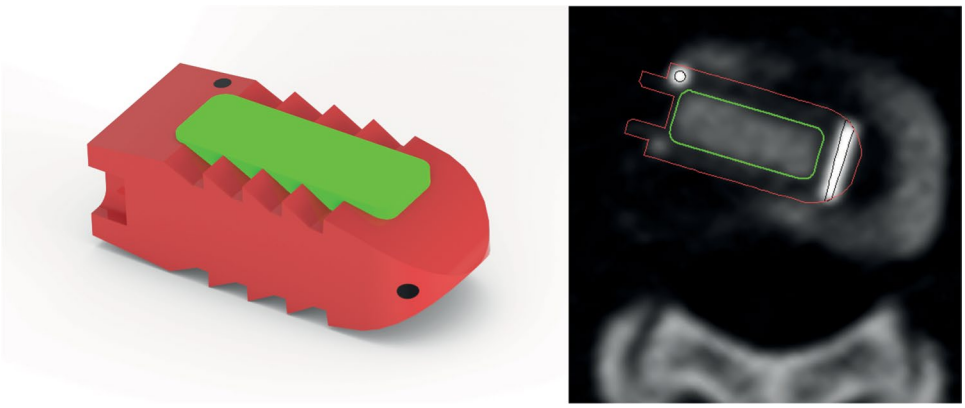

Fig. 1 Three-dimensional render of the polyether ether ketone (PEEK) cage design (red) including titanium markers (black) and graft window (green). Titanium markers were used to appropriately reposition the cage into each computed tomography (CT) scan

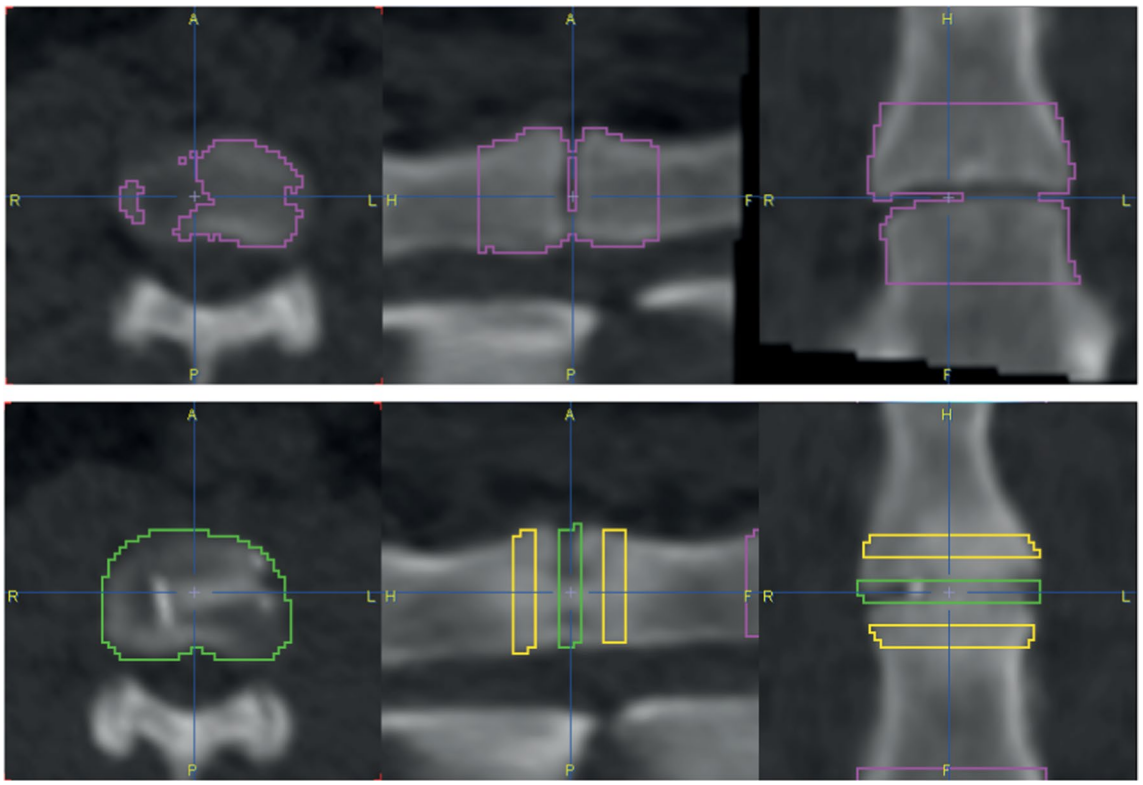

Fig. 2 Upper row shows the volume of interest of the reference (VOI_{REF}) at the unaffected segment L5–L6 in pink. Lower row displays the interbody and endplate volume of interest (VOI_{IB} and VOI_{EP}) at the operated segment in green and yellow, respectively

respectively. To prevent any edge effects from the interface of the cage and the vertebral bodies, VOI_{IB} and VOI_{EP} were drawn at a distance of 3.75 mm from each other (Fig. 2, lower row). These VOIs were transferred to the corresponding attenuation-corrected and normalized PET images to determine the mean and maximum normalized uptake values within these specific volumes. To express the relation between the normalized uptake value in VOI_{IB} and VOI_{EP}, the VOI_{IB} value was divided by the mean of the VOI_{EP} values above and below. The normalized activity in VOI_{IB} and the ratio of VOI_{IB} to VOI_{EP} were both plotted versus percentage of bone volume as derived from the diagnostic CT scans. A third-degree polynomial curve was fitted to the set of data points using MATLAB (MathWorks, Natick, MA, USA).

Histology

The isolated intervertebral segments were processed for undecalcified histology as described before [17]. In short, specimens were fixed in formalin, dehydrated through a series of ethanol, and polymerized with methyl methacrylate. Midsagittal sections of 20 µm were obtained and stained with basic fuchsin and methylene blue solutions to visualize mineralized tissue in and around the cage. An image of the cage region was digitalized using bright light microscopy.

Results

All sheep were longitudinally monitored according to protocol, so every sheep was scanned using PET/CT at 6 and 12 weeks after surgery. Figure 3 displays sagittal images of every diagnostic CT scan with a uniform grayscale across images. The bone volume inside the cage was graphically rendered and expressed as percentage below the images. Bone volumes varied largely between sheep and time points and covered nearly the whole spectrum of consolidation of interbody fusion, i.e. from hardly any bone volume (2% for scan a) to almost complete ossification of the graft window (86% for scan F). The amount of bone volume increased within every sheep between 6 and 12 weeks after surgery (lowercase versus uppercase letters). One of the sheep presented higher bone volume at 6 weeks after surgery (scan f) than all other five sheep at 12 weeks after surgery (scan A-E). In addition, the normalized attenuation-corrected ^{18}F-NaF PET sagittal images are shown in Fig. 3. Colors represent the normalized uptake value and, thus, indicate the amount of tracer uptake in that particular voxel with respect to the mean tracer uptake in the reference volume. Within the interbody and endplate volumes of the intervertebral segment, the tracer uptake fluctuated with increasing bone volume and could increase up to ten times the reference

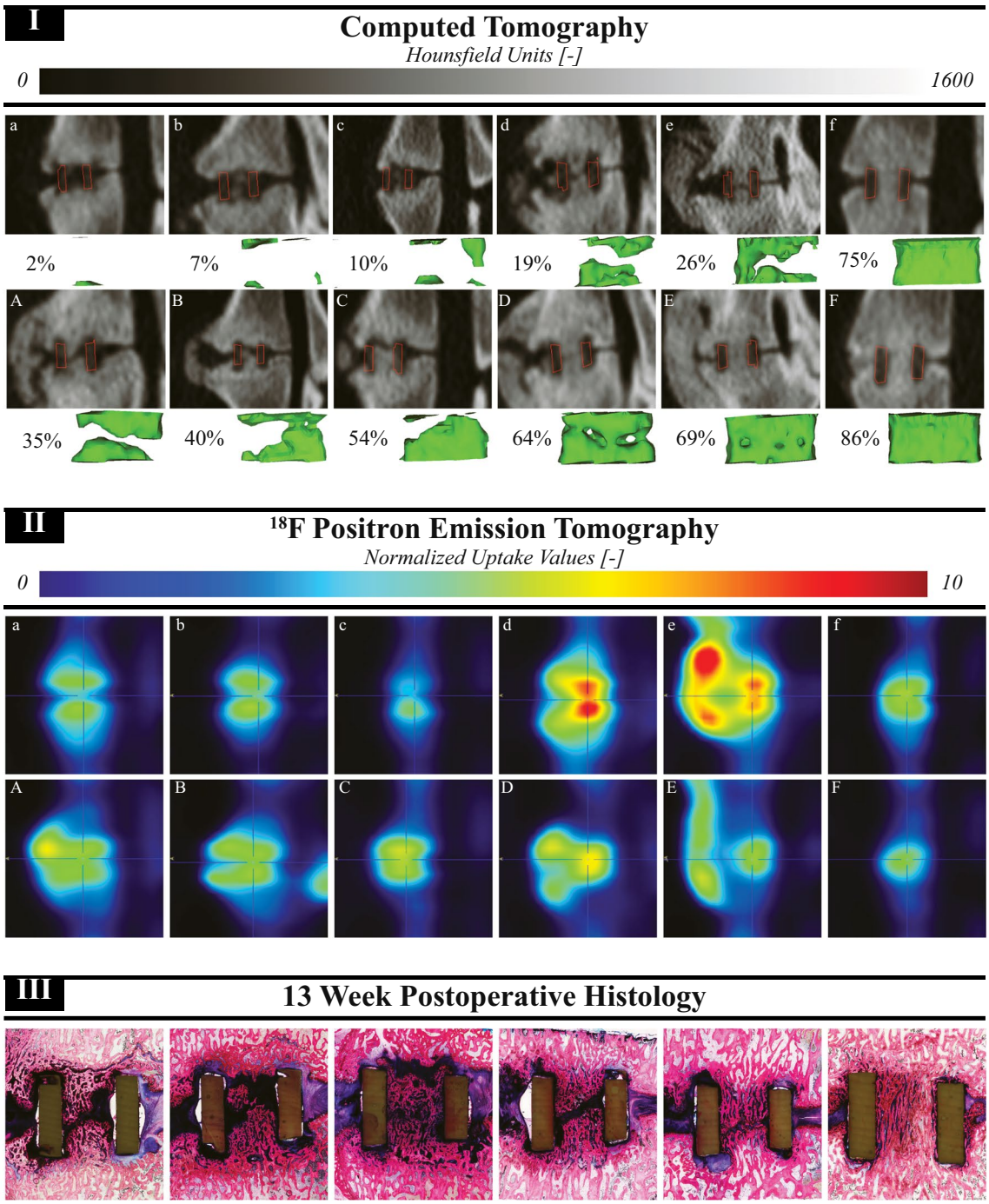

Fig. 3 Diagnostic computed tomography (CT) [panel I], ^{18}F sodium fluoride (^{18}F-NaF) positron emission tomography (PET) [panel II] sagittal images for each sheep (a-f) at 6 (lowercase) and 12 (uppercase) weeks after surgery. The contours of the polyether ether ketone (PEEK) cage are visualized in red in the CT scans. Additionally, the percentage bone volume and the three-dimensional render of the bone (in green) within the graft window are displayed per CT scan. Corresponding basic fuchsin and methylene blue sections, obtained 13 weeks postoperatively, are also displayed for each of the six sheep [panel III]. Orientation of images: top, cranial; bottom, caudal; left, anterior; right, posterior

uptake value. The further away from the surgical site, the more the normalized uptake value approached the value of one, meaning the tracer uptake in those voxels was equal to the mean tracer uptake in the reference volume. Both the CT and PET images revealed substantial anterolateral bone formation outside the PEEK cage in every sheep. In addition, the corresponding 13-week postoperative histologic midsagittal sections are displayed per sheep in Fig. 3. Per sheep,

the bone in the histologic section matches the anatomy of the bone as revealed by the 12-week postoperative CT data.

Figure 4 shows the mean (upper left) and maximum (lower left) normalized activity in the VOI_{IB} over percentage of bone within the graft window. When there was hardly any bone present within the graft window, the activity in the VOI_{IB} was relatively low. Both mean and maximum activity peaked at 25–40% of bone volume. At higher bone volumes, the activity declined again. For all data points, mean and maximum normalized activity values were continuously exceeding the value of one, i.e. the uptake values in the VOI_{IB} were found to be consistently higher than the mean activity of the VOI_{REF}. The ratio between the activity in the VOI_{IB} and the activity in the VOI_{EP} are shown at the right-hand side of Fig. 4. When there was a low amount of bone present within the graft window, the ratios were found to be lower than one, meaning the uptake in the VOI_{EP} was higher than in the VOI_{IB}. With increasing bone volume, the ratio approached and exceeded the value of one, indicating higher activity in the VOI_{IB} with respect to the activity in the VOI_{EP}.

Discussion

This study aimed to evaluate the changes in local bone metabolism as measured by ^{18}F-NaF PET/CT during the consolidation process of LIF in a sheep model. Although the local bone metabolism in the interbody region was consistently higher than the metabolism in reference bone, it strongly varied with interbody fusion status. With increasing bone volume in the cage, the bone metabolism in the interbody region was shown to increase, peak, and decrease after which it seemed to stabilize at an activity level above that of reference bone. This trend was found for both the mean and maximum bone metabolism within the interbody region.

In this study, a bell-shaped curve was found for the bone metabolism in the interbody region versus fusion status. The development of this characteristic curve can be related to the process of bone graft incorporation in interbody fusion, which is described to entail three distinct stages [19, 20]. First, there is an early inflammatory stage (hours–days) in which granulation tissue is formed and vascularized. Second, there is a repair stage (weeks-months) in which the original bone graft is resorbed and simultaneously replaced by new woven bone, a process called creeping substitution [21]. Third, the woven bone mass remodels (months–years) into lamellar bone with a trabecular architecture which adapts to the mechanical loads experienced by the tissue [22]. Within these three distinct stages, bone metabolism is the most active during creeping substitution in the repair stage. To achieve creeping substitution in the center of the interbody cage, bone progenitor cells must first migrate from the vertebral endplates towards the graft window of the cage [23]. Formation of new bone and vascular tissue, thus, commences at the endplates before it reaches the interbody

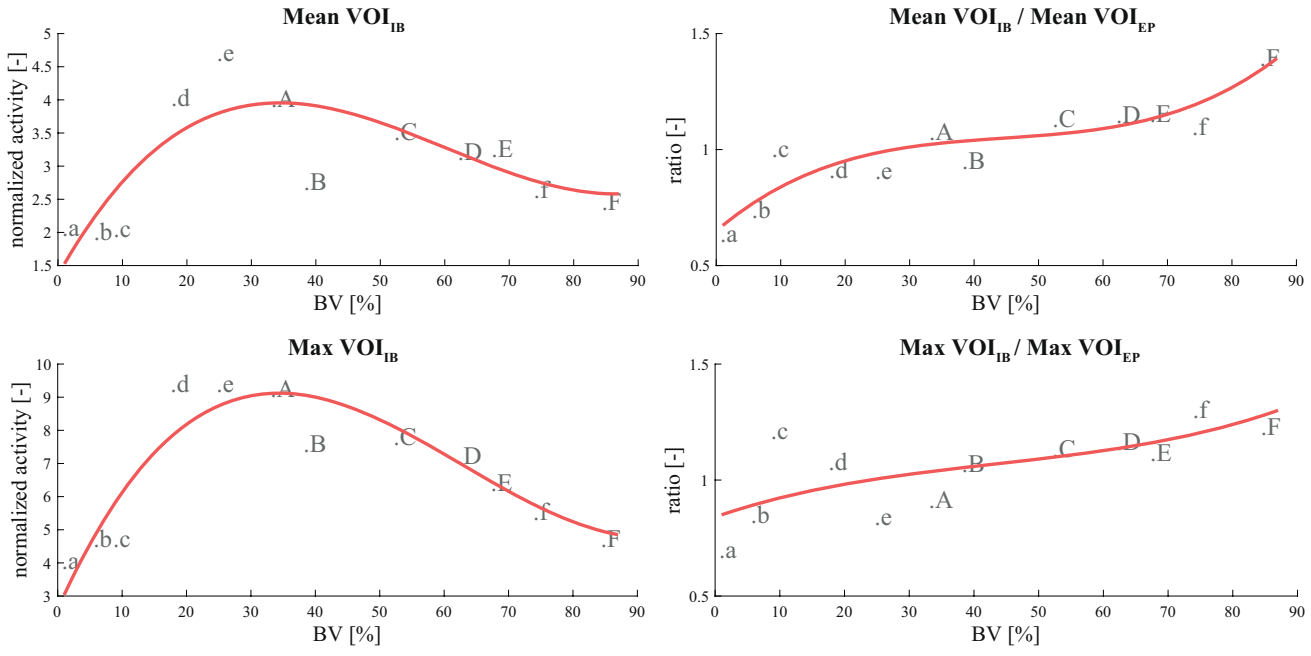

Fig. 4 For every scan, the activity in the VOI_{IB} and the ratio of the activity in the VOI_{IB} to the activity in the VOI_{EP} were plotted against percentage of bone volume (BV). Letters correspond to the individual scans as visualized and described in Fig. 3. A third-degree polynomial curve (in red) was fitted to these data points

region. For this reason, the bone metabolism was found to be higher in the endplate region than in the interbody region at the onset of fusion. Additionally, the initial absence of the bone progenitor cells in the interbody region explains the delayed increase that was found in this study for the ^{18}F-NaF uptake in the middle of the interbody region during consolidation of fusion. Once new bone formation at the endplates was achieved and a vascular connection between bone marrow and interbody region was established, bone progenitor cells could enter the interbody region, differentiate, and start to actively deposit new bone in the interbody region. As a result, the bone metabolism in the interbody region peaked and exceeded the bone metabolism in the endplate region as fusion progressed. Upon complete ossification of the graft window, bone metabolism in the interbody region decreased and stabilized at an activity still higher than that of unaffected bone. Thus, the fusion mass of the segment in which the fusion was most consolidated was still actively remodeling.

The method used to quantify the fusion status of each individual CT scan in this study yielded the percentage of bone volume within the graft window of the cage. This value described the percentage of bone inside the cage without considering the microarchitecture of the segmented bone volume. As a consequence, this quantification method would not be appropriate to analyze microstructural changes of the bone in the remodeling stage of the healing process. This was of no concern in the current study, as it focused on short postoperative time periods only and aimed to monitor the bone metabolism from surgery up until the remodeling stage. It should, however, be acknowledged that the quantification of cage bone volume is not a standard clinical procedure as it involves relatively high radiation exposure and time-consuming manual image processing. In clinical practice, the number of bony bridges through and around the cage is often scored instead [24, 25].

Because bone remodeling activity varied considerably between sheep and did not reveal a distinct trend between 6 and 12 weeks after surgery, the bone remodeling activity value of each individual PET scan was interpreted as a function of bone volume. Current analysis assumed that all sheep followed the same uncompromised progression of fusion, but with a different speed. To confirm this assumption, all sheep should have been monitored using PET/CT at regular (shorter) time intervals up until the remodeling stage of the healing process. This was, however, unattainable as the sheep originated from an existing cohort with a short postoperative time period. Monitoring each sheep at regular time intervals up until the remodeling stage would generate activity versus bone volume plots as in Fig. 4 per individual sheep, which would provide more insight in the time and subject dependency of the local bone metabolism in an operated segment.

The observed presence of anterolateral bone formation outside the PEEK cages in all animals may have resulted in inaccuracies in current analyses. First, tracer activity spillover from the anterolateral bone region outside the PEEK cage into the interbody region is expected due to limited spatial resolution in PET images [26]. Since the amount of spillover depends on the amount and distribution of activity in the anterolateral bone region, which varied across scans, it was difficult to correct for this spillover. However, it may have resulted in slight overestimations of the actual interbody tracer uptake. Second, the anterolateral bone formations may have stabilized the intervertebral segment once a complete bony bridge was developed between the two vertebrae. This stabilization might in turn have affected the formation of bone within the cage, as it has been shown before that additional stabilization of a spinal segment might increase the chances of intervertebral consolidation [27]. Anterolateral bone formation outside the cage has been reported before in ovine interbody fusion models [28]. In this study, the formation of these bony structures is, however, expected to mainly originate from the surgical rasping which preceded impaction of the cage into the disc space. Rasping might have promoted bone formation outside the interbody region as the procedure presumably stimulated the periosteum surrounding the vertebrae [29, 30]. The rasping and cage impaction procedure was included in current surgical technique to avoid the use of pins in the vertebral bodies for distraction, which is generally required for cage insertion. Insertion of vertebral pins would have led to increased bone remodeling within the vertebrae, which was unwanted since endplate regions were also of interest in our current analyses. For future research, if solely focusing on interbody bone metabolism, it would be interesting to perform vertebral distraction to open up the disc space instead of the gradual rasping and impaction procedure. We hypothesize that implementation of a distraction step could reduce the bone formation outside the interbody region, albeit at the expense of an increased background signal at the center of the vertebrae in which the distraction pins were inserted.

This study addressed the changes in local bone metabolism following LIF surgery and proposed the underlying processes responsible in an ovine model. Since loading conditions on the ovine spine resemble those of humans and ovine models accurately approach human bone remodeling and turnover [31, 32], the presented changes in local bone metabolism are believed to hold true for the human spine as well. However, the time scale of these changes might differ from the clinical situation as bony union is generally attained more rapidly in ovine models compared to human patients [33, 34]. The bell-curved development of bone metabolism in well-consolidating spinal segments suggests that short-term PET quantifications for prognostic diagnosis should not be too late after surgery. In the initial

phase of bone ingrowth an increased metabolic activity correlates with well-consolidating segments, whereas after this initial phase ambiguity arises as it becomes unknown whether the metabolic activity should still increase or should already decrease again. On long-term diagnostic follow-up (> years), this issue does not play part anymore as elevated bone metabolism has been recognized as a sign of micro-instability at this time scale [11, 15]. However, it is impossible to define a clear postoperative time point after which bone metabolism should reduce to homeostatic values again. Moreover, it remains hard to predict how markedly compromised segments will differ in bone metabolism from well-consolidating segments.

Previously, Foldager et al. revealed different metabolic patterns at 2, 4, and 8 weeks after surgery using PET quantifications in a porcine model in which PEEK interbody cages were enriched with autologous ICBG or osteobiologics [35]. Although their study proved that PET quantifications early after surgery could differentiate between two substantially different ossification mechanisms, changes in bone metabolism were not directly expressed in terms of progression of fusion The current study demonstrated the changes in local bone metabolism in a consolidating segment and clarified the variance in bone metabolism that may exist in well-fusing segments early after surgery. The location and intensity of the bone metabolism early after surgery provides additional information on the ongoing fusion process (prognostic) but should remain complementary to CT analysis (diagnostic) since early PET signals can be ambiguous on their own and can vary between subjects significantly. We believe it is important to take this variance into account, especially when interpreting PET signals of individual patients. Knowing the changes in local bone metabolism during uncompromised consolidation of spinal interbody fusion might enable identification of impaired bone formation early after LIF surgery using PET/CT quantifications. Early identification of impaired healing might aid in implementation of timely and efficient clinical measures potentially resulting in less non-unions. Future studies are warranted to investigate the exact timing and changes in local bone metabolism in the human spine following LIF surgery, and whether these changes may be affected by skeletal disorders (e.g. osteoporosis), by drug administration (e.g. parathyroid hormones, bone morphogenetic proteins), and by the combination of bone graft and cage material that is used.

Acknowledgements The authors are grateful to the Medanex Clinic team and all personnel of the Maastricht University animal facility for their help and expertise in performing animal studies. The authors would also like to thank the personnel of the department of Radiology and Nuclear Medicine for performing scanning procedures. Additionally, the authors would like to acknowledge Natasja van Dijk (Radboud University Medical Center, Nijmegen) for performing the histology.

Author contributions All authors contributed to the study conception and design. Material preparation, data collection and analysis were performed by AL, MP, and PW. The first draft of the manuscript was written by AL and all authors commented on previous versions of the manuscript. All authors read and approved the final manuscript.

Funding The research for this paper was financially supported by the Prosperos project, funded by the Interreg VA Flanders—the Netherlands program, CCI grant no. 2014TC16RFCB046.

Declarations

Conflict of interests All other authors have no conflicts of interest.

Ethical approval All animal protocols were conducted in accordance with the European directive 2010/63/EU and were approved by local animal welfare committees at the involved institutions in Belgium (Medanex Clinic, Diest; EC MxCl 2018–110) and the Netherlands (Maastricht University, Maastricht; AVD1070020185685).

References

1. Mobbs RJ, Phan K, Malham G, Seex K, Rao PJ (2015) Lumbar interbody fusion: techniques, indications and comparison of interbody fusion options including PLIF, TLIF, MI-TLIF, OLIF/ATP, LLIF and ALIF. J Spine Surg 1:2–18
2. Duarte RM, Varanda P, Reis RL, Duarte ARC, Correia-Pinto J (2017) Biomaterials and bioactive agents in spinal fusion. Tissue Eng Part B Rev 23:540–551
3. Meng B, Bunch J, Burton D, Wang J (2021) Lumbar interbody fusion: recent advances in surgical techniques and bone healing strategies. Eur Spine J 30:22–33
4. Raizman NM, O'Brien JR, Poehling-Monaghan KL, Yu WD (2009) Pseudarthrosis of the spine. J Am Acad Orthop Surg 17:494–503
5. Chun DS, Baker KC, Hsu WK (2015) Lumbar pseudarthrosis: a review of current diagnosis and treatment. Neurosurg Focus 39:E10
6. DePalma AF, Rothman RH (1968) The nature of pseudarthrosis. Clin Orthop Relat Res 59:113–118
7. Kornblum MB, Fischgrund JS, Herkowitz HN, Abraham DA, Berkower DL, Ditkoff JS (2004) Degenerative lumbar spondylolisthesis with spinal stenosis: a prospective long-term study comparing fusion and pseudarthrosis. Spine 29:726–733 (**Discussion 33-4**)
8. Peters MJM, Bastiaenen CHG, Brans BT, Weijers RE, Willems PC (2019) The diagnostic accuracy of imaging modalities to detect pseudarthrosis after spinal fusion-a systematic review and meta-analysis of the literature. Skelet Radiol 48:1499–1510
9. Fogel GR, Toohey JS, Neidre A, Brantigan JW (2008) Fusion assessment of posterior lumbar interbody fusion using radiolucent cages: X-ray films and helical computed tomography scans compared with surgical exploration of fusion. Spine J Off J N Am Spine Soc 8:570–577
10. Hawkins RA, Choi Y, Huang SC, Hoh CK, Dahlbom M, Schiepers C, Satyamurthy N, Barrio JR, Phelps ME (1992) Evaluation of the skeletal kinetics of fluorine-18-fluoride ion with PET. J Nucl Med Off Publ Soc Nucl Med 33:633–642
11. Fischer DR, Zweifel K, Treyer V, Hesselmann R, Johayem A, Stumpe KD, von Schulthess GK, Hany TF, Strobel K (2011) Assessment of successful incorporation of cages after cervical or lumbar intercorporal fusion with [(18)F]fluoride

positron-emission tomography/computed tomography. Eur Spine J Off Publ Eur Spine Soc Eur Spinal Deform Soc Eur Sect Cerv Spine Res Soc 20:640–648
12. Pouldar D, Bakshian S, Matthews R, Rao V, Manzano M, Dardashti S (2017) Utility of 18F sodium fluoride PET/CT imaging in the evaluation of postoperative pain following surgical spine fusion. Musculoskelet Surg 101:159–166
13. Genant HK, Bautovich GJ, Singh M, Lathrop KA, Harper PV (1974) Bone-seeking radionuclides: an in vivo study of factors affecting skeletal uptake. Radiology 113:373–382
14. Brenner W, Vernon C, Conrad EU, Eary JF (2004) Assessment of the metabolic activity of bone grafts with 18F-fluoride PET. Eur J Nucl Med Mol Imaging 31:1291–1298
15. Peters M, Willems P, Weijers R, Wierts R, Jutten L, Urbach C, Arts C, van Rhijn L, Brans B (2015) Pseudarthrosis after lumbar spinal fusion: the role of (18)F-fluoride PET/CT. Eur J Nucl Med Mol Imaging 42:1891–1898
16. Peters MJM (2019) The diagnostic potential of 18F-Fluoride PET/CT in lumbar spinal fusion patients—early detection of pseudarthrosis and identification of pain generators after surgery [Doctoral Thesis]. Maastricht University, Maastricht
17. Loenen ACY, Peters MJM, Bevers RTJ, Schaffrath C, van Haver E, Cuijpers V, Rademakers T, van Rietbergen B, Willems PC, Arts JJ (2021) Early bone ingrowth and segmental stability of a trussed titanium cage versus a polyether ether ketone cage in an ovine lumbar interbody fusion model. Spine J Off J N Am Spine Soc. https://doi.org/10.1016/j.spinee.2021.07.011
18. Parvizi N, Franklin JM, McGowan DR, Teoh EJ, Bradley KM, Gleeson FV (2015) Does a novel penalized likelihood reconstruction of 18F-FDG PET-CT improve signal-to-background in colorectal liver metastases? Eur J Radiol 84:1873–1878
19. Boden SD, Schimandle JH, Hutton WC (1995) An experimental lumbar intertransverse process spinal fusion model: radiographic, histologic, and biomechanical healing characteristics. Spine 20:412–420
20. Kalfas IH (2001) Principles of bone healing. Neurosurg Focus 10:E1
21. Burchardt H (1983) The biology of bone graft repair. Clin Orthop Relat Res 174:28–42
22. Smit TH, Muller R, van Dijk M, Wuisman PI (2003) Changes in bone architecture during spinal fusion: three years follow-up and the role of cage stiffness. Spine 28:1802–1808 (**Discussion 9**)
23. Craig Boatright K, Boden SD (2005) Biology of spine fusion. In: Lieberman JR, Friedlaender GE (eds) Bone regeneration and repair: biology and clinical applications. Humana Press, Totowa, pp 225–239
24. Burkus JK, Foley K, Haid RW, LeHuec JC (2001) Surgical Interbody Research Group–radiographic assessment of interbody fusion devices: fusion criteria for anterior lumbar interbody surgery. Neurosurg Focus 10:E11
25. Ajiboye RM, Hamamoto JT, Eckardt MA, Wang JC (2015) Clinical and radiographic outcomes of concentrated bone marrow aspirate with allograft and demineralized bone matrix for posterolateral and interbody lumbar fusion in elderly patients. Eur Spine J Off Publ Eur Spine Soc Eur Spinal Deform Soc Eur Sect Cerv Spine Res Soc 24:2567–2572
26. Soret M, Bacharach SL, Buvat I (2007) Partial-volume effect in PET tumor imaging. J Nucl Med Off Publ Soc Nucl Med 48:932–945
27. Anjarwalla NK, Morcom RK, Fraser RD (2006) Supplementary stabilization with anterior lumbar intervertebral fusion–a radiologic review. Spine 31:1281–1287
28. Steffen T, Stoll T, Arvinte T, Schenk RK (2001) Porous tricalcium phosphate and transforming growth factor used for anterior spine surgery. Eur Spine J Off Publ Eur Spine Soc Eur Spinal Deform Soc Eur Sect Cerv Spine Res Soc 10:S132–S140
29. Dwek JR (2010) The periosteum: what is it, where is it, and what mimics it in its absence? Skelet Radiol 39:319–323
30. Wu S, Lin Z, Yamaguchi A, Kasugai S (2015) The effects of periosteum removal on the osteocytes in mouse calvaria. Dent Oral Cranio-fac Res
31. Pearce AI, Richards RG, Milz S, Schneider E, Pearce SG (2007) Animal models for implant biomaterial research in bone: a review. Eur Cell Mater 13:1–10
32. Smit TH (2002) The use of a quadruped as an in vivo model for the study of the spine—biomechanical considerations. Eur Spine J Off Publ Eur Spine Soc Eur Spinal Deform Soc Eur Sect Cerv Spine Res Soc 11:137–144
33. Lindley EM, Barton C, Blount T, Burger EL, Cain CMJ, Seim HB, Turner AS, Patel VV (2017) An analysis of spine fusion outcomes in sheep pre-clinical models. Eur Spine J 26:228–239
34. Schiffman M, Brau SA, Henderson R, Gimmestad G (2003) Bilateral implantation of low-profile interbody fusion cages: subsidence, lordosis, and fusion analysis. Spine J Off J N Am Spine Soc 3:377–387
35. Foldager C, Bendtsen M, Zou X, Zou L, Olsen AK, Munk OL, Stodkilde-Jorgensen H, Bunger C (2008) ISSLS prize winner: positron emission tomography and magnetic resonance imaging for monitoring interbody fusion with equine bone protein extract, recombinant human bone morphogenetic protein-2, and autograft. Spine 33:2683–2690

Publisher's Note Springer Nature remains neutral with regard to jurisdictional claims in published maps and institutional affiliations.